Ultrafast direct laser writing of cladding waveguides in the $0.8CaSiO_3$-$0.2Ca_3(PO_4)_2$ eutectic glass doped with Nd^{3+} ions

J. Martínez de Mendívil,[1,a)] D. Sola,[2] J. R. Vázquez de Aldana,[3] G. Lifante,[1] A. H. de Aza,[4] P. Pena,[4] and J. I. Peña[2]
[1]*Departamento de Física de Materiales, C-04, Facultad de Ciencias, Universidad Autónoma de Madrid, 28.049 Madrid, Spain*
[2]*Departamento de Ciencia y Tecnología de Materiales y Fluidos, Instituto de Ciencia de Materiales de Aragón, Universidad de Zaragoza-CSIC, 50.018 Zaragoza, Spain*
[3]*Grupo de Investigación en Microprocesado de Materiales con Láser, Departamento de Física Aplicada, Universidad de Salamanca, 37.008 Salamanca, Spain*
[4]*Instituto de Cerámica y Vidrio-CSIC, 28.049 Madrid, Spain*

(Received 20 October 2014; accepted 17 January 2015; published online 28 January 2015)

We report on tubular cladding optical waveguides fabricated in Neodymium doped Wollastonite-Tricalcium Phosphate glass in the eutectic composition. The glass samples were prepared by melting the eutectic powder mixture in a Pt-Rh crucible at 1600 °C and pouring it in a preheated brass mould. Afterwards, the glass was annealed to relieve the inner stresses. Cladding waveguides were fabricated by focusing beneath the sample surface using a pulsed Ti:sapphire laser with a pulse-width of 120 fs working at 1 kHz. The optical properties of these waveguides have been assessed in terms of near-field intensity distribution and transmitted power, and these results have been compared to previously reported waveguides with double-line configuration. Optical properties have also been studied as function of the temperature. Heat treatments up to 700 °C were carried out to diminish colour centre losses where waveguide's modes and transmitted power were compared in order to establish the annealing temperature at which the optimal optical properties were reached. Laser experiments are in progress to evaluate the ability of the waveguides for 1064 nm laser light generation under 800 nm optical pumping. © *2015 AIP Publishing LLC*.
[http://dx.doi.org/10.1063/1.4906963]

I. INTRODUCTION

Ultrafast laser inscription (ULI) has demonstrated its feasibility and suitability throughout the last decade to fabricate three dimensional waveguides inside dielectric materials. Since the first work reported by Davis,[1] optical waveguides have been produced in a great variety of optical materials such as glasses and crystals, including rare-earth doped dielectric materials with the purpose of fabricating active integrated optical devices.[2–4]

Ultrafast laser inscription uses focused femtosecond laser pulses to induce a permanent positive or negative refractive index change in the focal volume of the dielectric media. When intense ultra-short laser pulses are tightly focused inside transparent materials, nonlinear absorption in the focal volume takes place, leading to different kinds of lattice damage, modifying the local refractive index and forming the so called "track" or "filament."[5] Waveguides produced by femtosecond laser inscription can be divided, up to date, into four categories depending on the characteristics in which the processing inscription is carried out.[6] There are some materials in which waveguiding can be observed directly in single written tracks, since the interaction between ultra-intense laser pulses and the material gives rise to a positive change in the refractive index. This is the case of several glasses and some crystals such as $LiNbO_3$,[7] and they are referred as Type I waveguides. Double-line configuration, the so-called Type II waveguides, is produced by scanning the laser focus along the sample producing two parallel damage tracks inside the sample. In this case, a refractive index decrease is generated in the damaged region by using energies above the optical breakdown threshold, being able to confine the light between the pair of tracks. Moreover, a refractive index increase in the central volume has been appreciated due to the stress induced during the irradiation. In Type III waveguides, also called cladding waveguides, a high refractive index region is produced by surrounding this volume with femtosecond damaged tracks. In Type IV waveguides, referred as ridge waveguides, high intensity pulses are used to etch selected regions through the ultrafast laser ablation. The fabrication of these types of waveguides has been studied along the last decade in crystalline and glassy matrices.[6–18]

With regards to the cladding waveguides, Type III, they are composed by the core, which is the nonirradiated region of the sample, and a surrounding cladding structure composed of several parallel tracks with reduced refractive index. The shape and the size of the cladding structure can be tailored and adjusted just by positioning the tracks adequately. These characteristics allow a better coupling to the waveguides, a low propagation loss, and a more efficient laser action in materials doped with Rare Earths (RE).[16–19] Nevertheless, it is important to note that for small cladding

a)Author to whom correspondence should be addressed. Electronic mail: jon.martinez@uam.es

waveguides, whose dimensions are in the order of the cladding structure, as the cladding waveguides reported in this work, there may exists an increase of the refractive index in the core due to the mechanical stress induced by the laser interaction with the glass.

In this work, we report on the fabrication of tubular shaped cladding waveguides by ultrafast laser inscription in $CaSiO_3$-$Ca_3(PO_4)_2$ eutectic glass doped with Nd^{3+} ions. The waveguiding properties have been evaluated for different processing conditions, and compared to the double-line configuration previously reported on this glass.[20] $CaSiO_3$-$Ca_3(PO_4)_2$ eutectic glass presents two interesting properties. First, it is a bioactive material since tricalcium phosphate (TCP), $Ca_3(PO_4)_2$, is osteoconductive and bioactive (reasorbable),[21] and wollastonite (W), $CaSiO_3$, is bioactive with osteostimulative properties.[22] Second, RE ions in this eutectic glass have excellent spectroscopic properties. In particular, lifetimes and emission cross-sections of the 1.06 μm (Nd^{3+}) and 1.5 μm (Er^{3+}) emissions in this glass are comparable to those of the best commercially used alkaline-silicate glasses.[23] Furthermore, it has been shown that its spectroscopic properties could be used as optical probe for biomedical applications.[24,25]

II. EXPERIMENTAL

A. Glass fabrication

The glass samples were obtained from the powder mixture of wollastonite (high-purity reagent-grade $CaSiO_3$, 99 wt. %, 200 mesh, Aldrich Chemistry, St. Louis, MO, USA) and synthesized tricalcium phosphate (purity > 99.9% and 1.50 Ca/P molar ratio, whose characteristics were reported elsewhere[26]) in the eutectic composition: 80% $CaSiO_3$, 20% $Ca_3(PO_4)_2$ expressed in mol. %. Furthermore, a 1 wt. % of Nd_2O_3 was added to the eutectic composite to obtain the doped samples. The resulting powders mixture was melted using a Pt-10 wt. % Rh crucible at 1600 °C in an electric furnace for 1 h to ensure a homogeneous liquid. The melt was poured onto a preheated brass mould obtaining a homogeneous, bubble-free, and transparent bulk glass. Afterwards, the glass was annealed at 795 °C for 30 min, and then slowly cooled down to room temperature in order to eliminate the stress formed during the fast cooling process after pouring the glass.

B. Waveguide fabrication

Cubic samples of $5 \times 5 \times 5\,mm^3$ were obtained by cutting the glass with a diamond blade. The surface to be processed was subsequently polished by means of sandpapers, increasing the grade from 800 up to 2500, and diamond polishing abrasives up to 0.25 μm. The cladding waveguides were fabricated by using a pulsed Ti:sapphire laser system that delivered transform limited 120 fs pulses with a central wavelength of 795 nm at a repetition rate of 1 kHz. Such repetition rate corresponds typically to the non-thermal processing regime[15] in which there are no heating accumulation effects in the sample due to the large temporal separation between consecutive pulses. The laser beam was focused by a 20× microscope objective (NA = 0.4), and the sample was placed in a XYZ motorized stage with spatial resolution of 0.2 μm. Different processing parameters were investigated to find the optimum conditions in terms of optical confinement and propagation losses. The geometrical focus was located either at 300 μm or at 600 μm beneath the surface of the sample, without seeing any relevant aberration problem due to the depth. The pulse energy was varied between 0.54 and 0.72 μJ with the help of a calibrated neutral density filter, a linear polarizer, and a half-wave plate. Under these conditions, parallel tracks were written with a lateral separation of 3 μm by scanning the piece at 500 μm/s. The polarization of the laser was kept in all the cases perpendicular to the scanning direction. The waveguide's diameter was varied between 20 and 150 μm. As an example, Figure 1 shows an optical microscope image of a 120 μm diameter waveguide at a depth of 600 μm beneath the surface, fabricated by using 0.72 μJ pulses, and with a separation between tracks of 3 μm.

In order to eliminate the absorption by colour centres induced during irradiation process, thermal treatments were carried out on the sample between 200 and 750 °C for 30 min, with heating/cooling rates of 900 °C/h.

C. Characterization techniques

The glass matrix composition was determined by means of scanning electron microscopy (SEM) using a field emission JEOL JSM-7000F microscope with EDX analysis. The amorphous character of the glass sample was confirmed by XRD analysis by using an XPert Pro MPD diffractometer.

Near-field intensity distribution of the waveguide's modes was characterized by using a He-Ne laser with 15 mW of output power, working in continuous mode emitting at 633 nm and using entrance and exit objectives DIN 20/0.40 and DIN 40/0.65, respectively, neutral filters with different transmittances, two polarizers, and a CCD camera.

Lifetime and luminescence measurements were performed by exciting the samples with a Ti:sapphire laser.

III. RESULTS AND DISCUSSION

Waveguides with diameters from 20 to 150 μm were characterized by means of near field intensity measurement

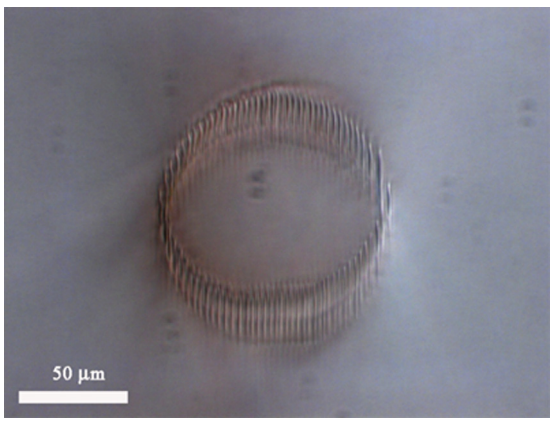

FIG. 1. Cross-section optical image of the Type III waveguides fabricated by fs laser writing with 0.72 μJ pulse energy.

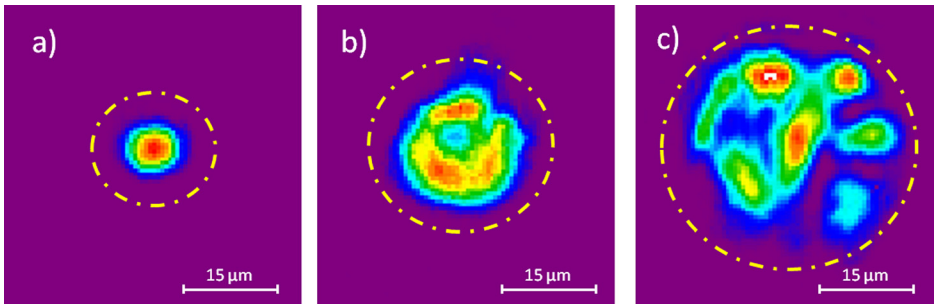

FIG. 2. Near-field intensity pattern of the TE mode of guides fabricated with 0.72 μJ pulse energy and diameters of 20, 30, and 40 μm.

and transmission losses analysis. Before any thermal treatment, near field modal analysis indicates good light confinement in all the waveguides, and a clear correspondence between the modal size and the dimensions of the waveguide structure created by the low-index barrier region induced by fs writing process. All the structures presented guided modes in quasi-TE and quasi-TM propagation at 633 nm, showing no remarkable differences dependent on the polarization, due to the relatively low index contrast in this type of guides. Only the 20 μm waveguide has been found to be monomode in both TE and TM polarizations. In consequence, only the waveguides with a diameter lower than 40 μm have been subjected to a more detailed analysis. Also, in the range of energies used in this work, no significant differences have been found for waveguides processed at different pulse energies. Figure 2 presents the transversal intensity distribution at the output for different waveguides, taken at 633 nm.

Following the procedure previously reported in double-line waveguides fabricated in this material with similar fabrication technique,[20] isochronal thermal treatments have been carried out in order to decrease the propagation losses by removing colour centres created in the waveguides during the laser writing process.[27–29] In this way, 30-min isochronal annealings have been applied starting from 200 °C up to 750 °C with steps of 50 °C. After each treatment, the propagation losses have been determined by measuring the transmitted power along the waveguide. Besides, the intensity distribution of the guided modes has been measured using a CCD camera.

Figure 3 shows the transmitted power of the 20, 30, and 40 μm waveguides after the thermal treatments as function of the annealing temperature. It can be observed a continuous improvement of the guiding light intensity for the three waveguides up to an annealing temperature of 500 °C. At this point, the transmitted optical power increases in a much more pronounced rate until a temperature of around 600 °C. The improvement on the transmitted power is as high as a factor 3 (compared to the values before any thermal treatment). The intensity at the output of the waveguides remains almost unaltered after the annealing at ~650 °C. Beyond this temperature, the propagation losses of the waveguides increase dramatically.

The behaviour of the transmitted power as a function of the annealing temperature can be understood by a combination of two processes: a gradual decrease of the colour centres and the partial recovery of the induced refractive index change. The improvement of the guided power until a processing temperature of ~600 °C could be explained by a continuous removal of colour centres, and even by releasing the stress generated during the fs-laser writing process. On the other hand, the smoothing of the damaged region should reduce scattering losses. The thermal treatments also readjust the structure in the zones modified by the laser writing process, and therefore induce a readjustment of the refractive index profile of the waveguide. For annealing temperatures higher than 650 °C, the optical barrier formed by the refractive index changes is reduced is such extent that tunnelling losses[30] become non-negligible. This extra mechanism of losses is expected to be responsible on the reduction of the transmitted power observed for temperatures beyond 650 °C.

Figure 4 presents the evolution of the FWHM of the mode intensity in the 20 μm diameter waveguide as function

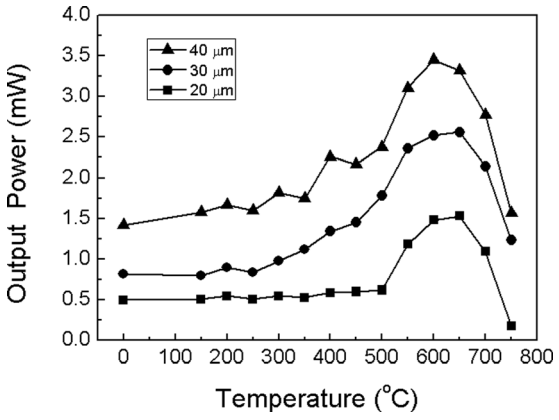

FIG. 3. Output power measured in guides with 20, 30, and 40 μm diameters, after heat treatments between 150 and 750 °C.

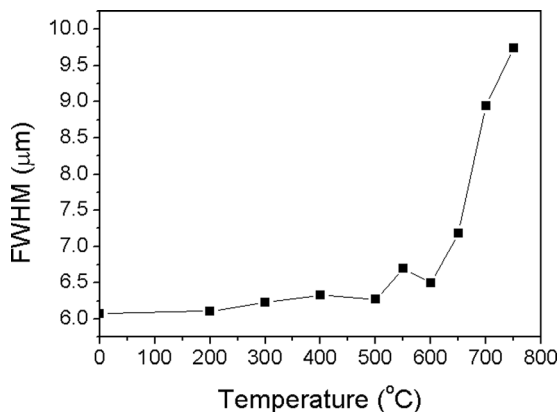

FIG. 4. Full width at half maximum of 20 μm waveguide TE mode, after each thermal treatment between 200 and 750 °C.

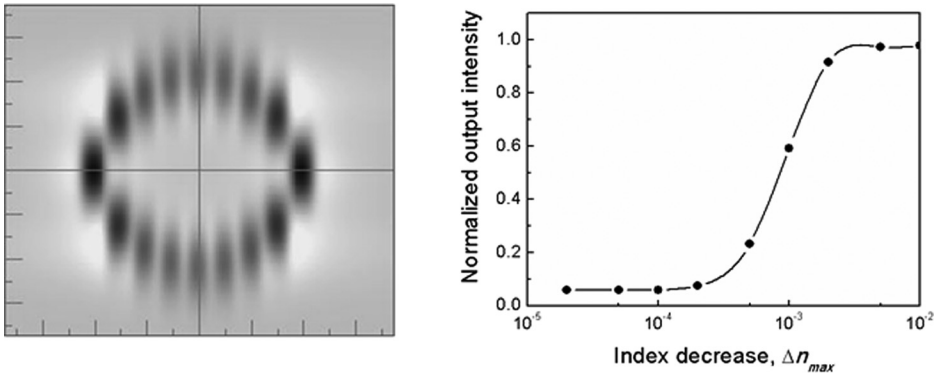

FIG. 5. Left: index profile of a 20 μm diameter waveguide for the 3D FD-BPM simulation. Right: modeled output intensity of the waveguide after 1 cm propagation length, in relation to the maximum refractive index modification generated by the fs-laser.

of the temperature treatments. The analysis of the modal intensity profiles reveals that the light confinement of the structure remains almost unaltered until an annealing temperature around 600 °C, while for higher temperature treatments, the data show clearly that the mode starts spreading. This temperature agrees with the temperature where the transmitted power started to decrease. These data are in accordance with the tunnelling losses mechanism suggested above.

Following this idea, the losses due to tunnelling process have been numerically evaluated in the frame of a 3D FD-BPM analysis. The 20 μm diameter waveguide structure has been modelled numerically and the propagation of the fundamental mode at 633 nm has been simulated. The refractive index profile used in the simulation is based on the index distribution generated by fs writing in Type II waveguides tracks.[31] The index modification for a single track centred at (0,0) is assumed to be

$$\Delta n = -\Delta n_{\max} \frac{1-(x/\sigma_x)^2}{1+(x/\sigma_x)^4} \exp\left(-y/\sigma_y\right)^2, \qquad (1)$$

where Δn_{max} is the maximum reduction on the refractive index in the track, and σ_x and σ_y are the width of the damaged region along the horizontal and vertical directions, respectively. While Δn_{max} depends on the laser pulse conditions, σ_x and σ_y are related with the beam waist and the focus depth of the focused beam inside the material, respectively. Figure 5 (left) shows the refractive index map used in the simulations, which is formed by 16 tracks centred along a circle of 10 μm of radius, with $\sigma_x = 1.5$ μm and $\sigma_y = 4$ μm. The losses due to the tunnelling trough the optical barriers formed by the tracks are evaluated by computing the power of the fundamental mode that remains inside the structure after 1 cm of propagation, as function of the maximum refractive index change Δn_{max}, as shown in Figure 5 (right). The numerical results indicate that a refractive index modification greater than 5×10^{-3} confines adequately the light in the structure. The guiding properties decay dramatically for index decrease lower than 3×10^{-3}, and for Δn_{max} lower than 5×10^{-4} the tunnelling losses are too high to properly sustain light propagation in the structure. These values agree with the increase in refractive index modifications reported in this material,[20] as well as the values reported in other materials with similar fabrication process.[2,32]

Comparing the experimental results of Figure 4 with the numerical simulations, it is possible to conclude that the index modification induced by the fs-laser processing induced at least an index change of 5×10^{-3}, which remains unaltered until thermal treatments at 600 °C. Annealing temperatures higher than 650 °C should recover the original matrix, destroying the index modifications, and thus the capability of light confinement inside the structure.

Comparing these waveguides to double track waveguides fabricated in $CaSiO_3$-$Ca_3(PO_4)_2$ as previously reported,[20] it can be noticed that it is possible to achieve higher temperatures during the thermal treatments without losing guiding properties. This point suggest that the tailoring of the waveguide allows to maintain the mode confined with a lower index increase, and thus, it is possible to improve the quality of the waveguides by applying more aggressive thermal treatments that in the case of the double filament waveguides lead to the destruction of the waveguide.[20] It is remarkable that Type II waveguides started to present propagation loses due to tunneling processes at 350 °C, while in the case of Type III waveguides, the quality of the waveguides improves continuously reaching the optimum point in de region between 600 and 650 °C.

Finally, the spectroscopic analysis of the Nd^{3+} ion inside the waveguides has been performed. It has been found that the luminescence spectra of the $^4F_{3/2} \rightarrow {}^4I_{11/2}$ transition presents no significant variations compared to the luminescence measured in bulk, as it can be seen in Figure 6. Lifetime of the $^4F_{3/2} \rightarrow {}^4I_{11/2}$ transition was also measured, obtaining a value of $\tau = 244$ μs, which is almost coincident

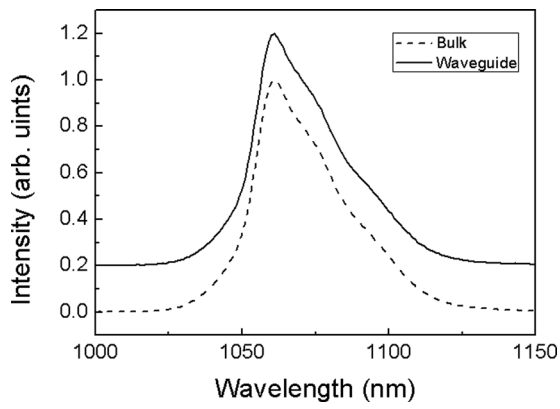

FIG. 6. Emission of Nd^{3+} at 1060 nm under excitation at 808 nm, collected from the bulk (dashed line) and from the fs-laser written waveguide (continuous line).

with the lifetime value of $\tau = 250\,\mu$s as previously reported in bulk.[20] These data indicate that the spectroscopic properties of the rare earth ions inside the waveguide core are almost unaffected by the fs-laser processing, thus making this doped material a good candidate for active integrated devices.

IV. CONCLUSIONS

The high optical quality Nd^{3+} doped $CaSiO_3$-$Ca_3(PO_4)_2$ eutectic glass samples have been manufactured by the casting technique. With the obtained samples, waveguides with different dimensions have been successfully fabricated by fs-laser writing technique. It has been found that the waveguides with diameters from 20 μm to 150 μm fabricated following this technique support TE and TM polarizations at 633 nm wavelength, and little influence of the pulse energy has been found. Isochronal thermal treatments have been carried out, where it was observed an improvement in the transmitted power up to a 300% after an annealing temperature of 600 °C. This improvement is associated to a decrease of absorption losses due to colour centres, a release of the stress generated during the waveguide fabrication process, and a decrease of the scattering losses by smoothing the damaged region. Up to this temperature, no significant modification in the modal intensity distribution was appreciated. It was also determined that for annealing temperatures higher than 650 °C, the waveguides started losing their confining properties due to tunnelling losses. The experimental results have been compared with numerical simulations using 3D FD-BPM. This analysis suggests a refractive index modification in the range of 5×10^{-3} before thermal treatment, and an index modification around 3×10^{-3} after the annealing at 650 °C. For lower index modification, the numerical modelling indicates an abrupt increase of the tunnelling losses which is in accordance with the experimental results. Finally, it has been found that the spectroscopic properties of the Nd^{3+} ion in the $CaSiO_3$-$Ca_3(PO_4)_2$ eutectic glass remain unaltered inside the waveguides core, which make these structures suitable for the development of integrated active devices.

ACKNOWLEDGMENTS

This work has been partially supported by the projects MAT2013-48426-C2-1-R, DISFOTINT (MECC, TEC2010-21574-C02-01/02) and MICROSERES (Comunidad de Madrid, P2009/TIC-1476).

Dr. Daniel Sola thanks the Bosch and Siemens Home Appliances Group, the 7th Framework Programme EU No 314630-UV Marking and MAT2013-41045-R for the financial support of his contract.

[1]K. M. Davis, K. Miura, N. Sugimoto, and K. Hirao, Opt. Lett. **21**, 1729 (1996).
[2]S. Nolte, M. Will, J. Burghoff, and A. Tuennermann, Appl. Phys. A **77**, 109 (2003).
[3]S. Taccheo, G. D. Valle, R. Osellame, G. Cerullo, N. Chiodo, P. Laporta, O. Svelto, A. Killi, U. Morgner, M. Lederer, and D. Kopf, Opt. Lett. **29**(22), 2626 (2004).
[4]R. R. Thomson, H. T. Bookey, N. D. Psaila, A. Fender, S. Campbell, W. N. MacPherson, J. S. Barton, D. T. Reid, and A. K. Kar, Opt. Express **15**, 11691–11697 (2007).
[5]H. Misawa and S. Juodkazis, *3D Laser Microfabrication. Principles and Applications* (Wiley, Weinheim, 2006).
[6]F. Chen and J. R. Vazquez de Aldana, Laser Photonics Rev. **8**, 251 (2014).
[7]G. Zhou and M. Gu, Appl. Phys. Lett. **87**, 241107 (2005).
[8]G. Zhou and M. Gu, Opt. Lett. **31**, 2783 (2006).
[9]J. Burghoff, S. Nolte, and A. Tunnermann, Appl. Phys. A **89**, 127 (2007).
[10]N. D. Psaila, R. R. Thomson, H. T. Bookey, A. K. Kar, N. Chiodo, R. Osellame, G. Cerullo, A. Jha, and S. Shen, Appl. Phys. Lett. **90**, 131102 (2007).
[11]G. A. Torchia, A. Ródenas, A. Benayas, E. Cantelar, L. Roso, and D. Jaque, Appl. Phys. Lett. **92**, 111103 (2008).
[12]J. Siebenmorgen, K. Petermann, G. Huber, K. Rademaker, S. Nolte, and A. Tünnermann, Appl. Phys. B **97**, 251 (2009).
[13]W. F. Silva, C. Jacinto, A. Benayas, J. R. Vazquez de Aldana, G. A. Torchia, F. Chen, Y. Tan, and D. Jaque, Opt. Lett. **35**(7), 916 (2010).
[14]L. B. Fletcher, J. J. Witcher, N. Troy, S. T. Reis, R. K. Brow, R. M. Vazquez, R. Osellame, and D. M. Krol, Opt. Mater. Express **1**(5), 845 (2011).
[15]A. Benayas, W. F. Silva, A. Ródenas, C. Jacinto, J. V. de Aldana, F. Chen, Y. Tan, R. R. Thomsom, N. D. Psaila, D. T. Red, G. A. Torchia, A. K. Kar, and D. Jaque, Appl. Phys. A **104**, 301 (2011).
[16]A. Okhrimchuk, V. Mezentsev, A. Shestakov, and I. Bennion, Opt. Express **20**, 3832 (2011).
[17]Y. Ren, G. Brown, A. Ródenas, S. Beecher, F. Chen, and A. K. Kar, Opt. Lett. **37**(16), 3339 (2012).
[18]A. G. Okhrimchuk, A. V. Shestakov, I. Khrushchev, and J. Mitchell, Opt. Lett. **30**(17), 2248 (2005).
[19]Q. An, Y. Jia, H. Liu, J. R. V. de Aldana, and F. Chen, Opt. Laser Technol. **56**, 382 (2014).
[20]D. Sola, J. M. de Mendívil, J. R. V. de Aldana, G. Lifante, R. Balda, A. H. de Aza, P. Pena, and J. Fernandez, Appl. Surf. Sci. **278**, 289 (2013).
[21]R. G. Carrodeguas and S. de Aza, Acta Biomater. **7**(10), 3536 (2011).
[22]R. G. Carrodeguas and P. N. de Aza, Bol. Soc. Esp. Ceram. Vidr. **50**(6), 301 (2011).
[23]J. A. Pardo, J. I. Peña, R. I. Merino, R. Cases, A. Larrea, and V. M. Orera, J. Non-Cryst. Solids **298**, 23 (2002).
[24]D. Sola, R. Balda, M. Al-Saleh, J. I. Peña, and J. Fernandez, Opt. Express **21**, 6561 (2013).
[25]D. Sola, R. Balda, J. I. Peña, and J. Fernandez, Opt. Express **20**(10), 10701 (2012).
[26]M. Magallanes-Perdomo, P. Pena, P. N. de Aza, R. G. Carrodeguas, M. A. Rodríguez, X. Turrillas, S. de Aza, and A. H. de Aza, Acta Biomater. **5**(8), 3057 (2009).
[27]P. Dekker, M. Ams, G. D. Marshall, D. J. Little, and M. J. Withford, Opt. Express **18**(4), 3274 (2010).
[28]A. Benayas, D. Jaque, B. McMillen, and K. P. Chen, J. Appl. Phys. **107**(3), 033522 (2010).
[29]M. E. Sanchez-Morales, G. V. Vazquez, G. Lifante, E. Cantelar, J. Rickards, and R. Trejo-Luna, Opt. Spectrosc. **110**(6), 885 (2011).
[30]P. D. Townsend, P. J. Chandler, and L. Zhang, *Optical Effects on Ion Implantation* (Cambridge Studies in Modern Optics Ed., 1994).
[31]A. Ródenas, L. M. Maestro, M. O. Ramírez, G. A. Torchia, L. Roso, F. Chen, and D. Jaque, Appl. Phys. **106**(1), 013110 (2009).
[32]A. Ródenas, G. A. Torchia, G. Lifante, E. Cantelar, J. Lamela, F. Jaque, L. Roso, and D. Jaque, Appl. Phys. B **95**(1), 85 (2009).